Synthesis, Optical, and Electrical Characterization of Organically Soluble Silver Nanoparticles and Their Poly(3-hexylthiophene) Nanocomposites: Enhanced Luminescence Property in the Nanocomposite Thin Films

Biplab K. Kuila, Ashesh Garai, and Arun K. Nandi*

Polymer Science Unit, Indian Association for the Cultivation of Science, Jadavpur, Kolkata, 700 032, India

Received July 26, 2007. Revised Manuscript Received September 1, 2007

The hexadecyl amine capped Ag nanoparticles in chloroform are prepared by reducing [Ag(hexadecyl amine)$_2$]NO_3 complex with sodium borohydride in a chloroform/water medium. Poly(3-hexyl thiophene) (P3HT)−silver nanoparticle composites at five different compositions [Ag10, Ag25, Ag50, Ag75, and Ag90; the number indicates percentage (w/w) of silver in the composite] are prepared by mixing the chloroform solutions of P3HT and hexadecyl amine capped Ag nanoparticles at appropriate proportions. Thin films (average thickness ∼ 50 nm) of the composites were prepared by spin-coating the above homogeneous solutions at 2000 rpm. The UV−vis spectra of the composite solutions exhibit a homogeneous mixing of the components as an intermediate absorption peak of those of the plasmon band of Ag and $\pi-\pi^*$ transition band of P3HT are observed in all cases. But the thin films retain the individual plasmon peak of Ag nanoparticle and the $\pi-\pi^*$ transition band of P3HT, showing a small red shift in both peaks at certain compositions. The TEM pictures indicate hexagonal array of Ag nanoparticles in the pure hexadecyl amine capped Ag nanoparticle film, but in the composites the Ag nanoparticles are distributed homogeneously. The histograms indicate an increase in nanoparticle size with increasing nanoparticle concentration and AFM study indicates cluster formation by organization of P3HT lamella surrounding the Ag nanoparticles. The photoluminescence spectra in the solution state shows a continuous decrease of luminescence intensity with increase in Ag nanoparticle concentration but the thin films of the nanocomposite indicate a significant (∼4 times for Ag50 and on considering P3HT concentration only it is an 8 times increase compared to that of pure P3HT) increase in fluorescence intensity. A small blue shift of the luminescence band of P3HT with increasing Ag nanoparticle concentration is also observed possibly for the coupling of plasmon vibration with the electronic levels of the excitons of P3HT. The pure hexadecyl amine capped Ag nanoparticles thin film exhibits electrical bistability, signifying switching effect in the system but the nanocomposite thin films do not show these characteristics. They show a sharp increase in current at a threshold voltage, which increase with an increase in Ag nanoparticle concentration except for the Ag75 composite. The characteristics of $I-V$ curves of the nanocomposites promise the probable use of nanocomposite thin films as efficient light-emitting diode compared to that of pure P3HT.

Introduction

Recently, research on metal colloids is greatly stimulated due to the unique properties of nanoscopic materials in optical, magnetic, and catalytic activities, which are different from those of bulk metals.[1−5] Investigation of the optical properties of silver nanoparticles is very interesting since the silver nanoparticles strongly absorb in the visible region due to their surface plasmon resonance.[6] Silver colloidal particles play important roles as substrates in the studies of surface-enhanced Raman scattering[7−9] and catalysis.[10] The synthesis of metal nanoparticles in an organic medium is important due to its enormous application in the field of ordered arrays of metallic nanoparticles, organic molecule protected nanoparticle thin film, and making of polymer nanoparticle composite.[10] Ordered arrays of the nanoparticles and their thin films are very important for their potential use in different fields like single-electron circuits,[11] memory devices,[12] chemical sensing,[13] catalysis,[10] and optoelectronic nanodevices.[14,15]

* To whom correspondence should be addressed. E-mail: psuakn@mahendra.iacs.res.in.

(1) Schmid, G. *Chem. Rev.* **1992**, *92*, 1709.
(2) Hanamura, E. *Phys. Rev. B* **1988**, *37*, 1273.
(3) Sun, T.; Seff, K. *Chem. Rev.* **1994**, *94*, 857.
(4) Ozin, G. A. *Adv. Mater.* **1992**, *4*, 612.
(5) Ershov, B. G.; Henglein, A. *J. Phys. Chem.* **1993**, *97*, 3434.
(6) Kapoor, S. *Langmuir* **1998**, *14*, 1021.
(7) Brandt, E. S.; Cotton, T. M. In *Investigations of Surfaces and Interfaces-Part B*, 2nd ed.; Rossiter, B. W., Baetzold, R. C., Eds.; John Wiley & Sons: New York, 1993; Vol. IXB, p 633.
(8) Nie, S. N.; Emery, S. R. *Science* **1997**, *275*, 1102.
(9) Nickel, U.; Castell, A. Z.; Pöppl, K.; Schneider, S. *Langmuir* **2000**, *16*, 9087.
(10) Shiraishi, Y.; Toshima, N. *J. Mol. Catal. A*: *Chem.* **1999**, *141*, 187.
(11) (a) Pantelides, S. T.; Reed, M. A.; Murday, J. A.; Aviram, A. *Mol. Electron., Mater. Res. Soc. Symp. Proc.* **1999**, *582*. (b) Averin, D. V.; Likharev, K. K. In *Single Electron Tunneling*; Grabert, H., Devoret, M. H., Eds., Plenum: New York, 1992; p 311.

10.1021/cm7020214 CCC: $37.00
Published on Web 10/05/2007

There are many methods for the synthesis of silver nanoparticles in an organic medium employing *n*-alkane thiol for stabilization of nanoparticles.[16] Also, the organic molecules containing amine functional groups form stable colloids. There are a few reports on the formation of the metal nanoparticle using a metal complex, which act as a metal ion provider as well as stabilizer including synthesis of silver nanoparticles using bidentate amine ligand like *N*-hexadecylethylenediamine.[17] Most of the work deals with the chemical and physical characterization including optical, FTIR, TEM, and SAXS to understand the ordering of the particle. As per our knowledge, no electrical and optical characterization of the thin films of amine capped silver nanoparticles yet have been done. In this paper we have used a long chain amine (hexadecyl amine) as the complexing ligand as well as stabilizer to produce silver nanoparticles and we have fully characterized the silver nanoparticle in the solution and solid state. Their electrical and optical properties in the ultrathin film state are carefully investigated.

The conducting polymer nanoparticle−composite films are of high interest due to their novel properties like luminescence,[18a] electro-active property,[18b] semiconducting behavior,[18c−e,19] and their applications in field effect transistors (FETs),[20] light-emitting diodes (LEDs),[18a] photovoltaic cells,[21] etc. The inclusion of the nanostructured material like clay,[22,23] multiwalled carbon nanotubes,[24] fullerenes,[25] and metafullerenes[26] in the conjugated polymer (CP) has been reported to affect the photoluminescence (PL) of the polymer. The quenching occurs due to the increase in exciton dissociation resulting from the photoinduced electron transfer from the photoexcited CP to the dopant and this effect has been used to improve the efficiency of the photovoltaic devices.[26] However, there are also reports where there is photoluminescence enhancement in the CP nanocomposites.[23,27] Composites of CPs and nanoparticles (NPs) have been extensively used as a means of retarding photo-oxidation of the polymer.[28] The triplet excitons of the luminescent polymers are quenched because of the overlap of their energy levels with the optical absorption of the added nanoparticle preventing photo-oxidation.[27,28] For this it is advantageous to have a uniform dispersion of the NPs within the host polymer matrix. Poly(3-hexyl thiophene) (P3HT), widely used in many applications like photovoltaic devices and LEDs, is of particular interest due to its self-organizing property to form a lamellar crystalline structure.[22,23] The optical, luminescence, and electrical properties, i.e., the mobility of the hole and electron, are very much dependent on regioregularity, molecular weight, homogeneity, and morphology of the film.[29−31]

Here, we have synthesized hexadecyl amine capped silver nanoparticles in a chloroform medium to incorporate the nanostructure in the P3HT matrix. We have used the long-chain amine as a complexing ligand as well as stabilizer to protect the aggregation of the silver nanoparticle in the polymer matrix. The long-chain amine cap of the nanoparticles may also help make the polymer compatible with the nanoparticle through dispersion interaction and may induce uniform dispersion of NPs in the polymer matrix. We have studied the UV−vis and fluorescence properties of the composite both in the solution and in ultrathin film to know whether there is any difference of these properties in the two states. Another major aim of our work is to investigate the electrical properties of nanoparticle assembled thin films of both pure silver nanoparticle and the nanocomposite as the electrical properties of nanoparticles/nanocomposites are different from those of the bulk materials.[23,24,32]

Experimental Section

(a) Synthesis of Hexadecyl Amine Silver(I) Nitrate. A solution of 7.2438 g of hexadecyl amine in 100 mL of water:ethanol (2:3 in volume) mixture was added with stirring to a solution of 1.6987 g of $AgNO_3$ in 100 mL of water:ethanol (2:3 in volume) mixture.[33a−d] The stirring was continued for 2 h and the final reaction composition was a 1:3 molar ratio of metal salt/hexadecyl amine. After evaporation of the solvent, the crude [Ag(hexadecyl

(12) Ouyang, J.; Chu, C.-W.; Sieves, D.; Yang, Y. *Appl. Phys. Lett.* **2005**, *86*, 123507.
(13) (a) Sharma, S.; Nirkhe, C.; Pethkar, S.; Athawale, A. A. *Sens. Actuators, B* **2002**, *85*, 131. (b) Majumdar, G.; Goswami, M.; Sarma, T. K.; Paul, A.; Chattopadhyay, A. *Langmuir* **2005**, *21*, 1663.
(14) Hickman, J. J.; Ofer, D.; Laibinis, P. E.; Whitesides, G. M.; Wrighton, M. S. *Science* **1991**, *252*, 688.
(15) Chen, S.; Ingram, R. S.; Hostetler, M. J.; Pietron, J. J.; Murray, R. W.; Schaaff, T. G.; Khoury, J. T.; Alvarez, M. M.; Whetten, R. L. *Science* **1998**, *280*, 2098.
(16) Chen, M.; Diao, G. W.; Li, C. H.; Jhu, X. M. *Nanotechnology* **2007**, *18*, 175706.
(17) Manna, A.; Imae, T.; Iida, M.; Hisamatsu, N. *Langmuir* **2001**, *17*, 6000.
(18) (a) Kukhta, A. V.; Kolesnik, E. E.; Lesnikovich, A. I.; Nichick, M. N.; Ritchik, D. V.; Vorobyova, S. A. *Mater. Sci. Eng. C* **2006**, *26*, 1012. (b) Kukhta, A. V.; Kolesnik, E. E.; Lesnikovich, A. I.; Nichick, M. N.; Kudlash, A. N.; Vorobyova, S. A. *Synth. React. Inorg. Metal-Org. Nano-Metal Chem.* **2007**, *37*, 333. (c) Greenham, N. C.; Brown, A. R.; Bradley, D. D. C.; Friend, R. H. *Synth. Met.* **1993**, *55−57*, 4134. (d) Oliveira, M. M.; Castro, E. G.; Canestraro, C. D.; Zanchet, D.; Ugarte, D.; Roman, L. S.; Zarbin, A. J. G. *J. Phys. Chem. B* **2006**, *110*, 17063. (e) Pinter, E.; Patakfalvi, R.; Fulei, T.; Gingl, Z.; Dekany, I.; Visy, C. *J. Phys. Chem. B* **2005**, *109*, 17474.
(19) McCullough, R. D.; Ewbank, P. C. In *Handbook of Conducting Polymers*, 2nd ed.; Skotheim, T. A., Elsebaumer, R. L., Reynolds, J. R., Eds.; Marcel Dekker: New York, 1998; p 225.
(20) Sandberg, H. G. O.; Frey, G. L.; Maxim, N.; Shkunov, M. N.; Sirringhaus, H.; Friend, R. H. *Langmuir* **2002**, *18*, 10176.
(21) Coakley, K. M.; McGehee, M. D. *Chem. Mater.* **2004**, *16*, 4533.
(22) Kuila, B. K.; Nandi, A. K. *Macromolecules* **2004**, *37*, 8577.
(23) Kuila, B. K.; Nandi, A. K. *J. Phys. Chem. B* **2006**, *110*, 1621.
(24) Kuila, B. K.; Malik, S.; Batabyal, S. K.; Nandi, A. K. *Macromolecules* **2007**, *40*, 278.
(25) Feldrapp, K.; Brutting, W.; Schwoerer, M.; Brettreich, M.; Hirsch, A. *Synth. Met.* **1999**, *101*, 156.
(26) Yang, S.; Fan, L.; Yang, S. *Chem. Phys. Lett.* **2004**, *388*, 253.
(27) Nicholson, P. G.; Ruiz, V.; Macpherson, J. V.; Unwin, P. R. *Chem. Commun.* **2005**, 1052.
(28) Park, J. H.; Lim, Y. T.; Park, O. O.; Kim, J. K.; Yu, J.-W.; Kim, Y. C. *Chem. Mater.* **2004**, *16*, 688.
(29) Sirringhaus, H.; Brown, P. J.; Friend, R. H.; Nielsen, M. M.; Bechgaard, K.; Langeveld-Voss, B. M. W.; Spiering, A. J. H.; Janssen, R. A. J.; Meijer, E. W.; Herwig, P.; de Leeuw, D. M. *Nature* **1999**, *401*, 685.
(30) Kline, R. J.; McGehee, M. D.; Kadnikova, E. N.; Liu, J.; Frechet, J. M. J. *Adv. Mater.* **2003**, *15*, 1519.
(31) Chang, J.-F.; Sun, B.; Breiby, D. W.; Nielsen, M. M.; Solling, T. I.; Giles, M.; McCulloch, I.; Sirringhaus, H. *Chem. Mater.* **2004**, *16*, 4772.
(32) (a) Malik, S.; Batabyal, S. K.; Basu, C.; Nandi, A. K. *J. Mater. Sci.* **2003**, *22*, 1113. (b) Bhattacharyya, S.; Malik, S.; Nandi, A. K.; Ghosh, A. *J. Chem. Phys.* **2006**, *125*, 174717.
(33) (a) Iida, M.; Yonezawa, A.; Tanaka, J. *Chem. Lett.* **1997**, 663. (b) Iida, M.; Tanase, T.; Asaoka, N.; Nakanishi, A. *Chem. Lett.* **1998**, 1275. (c) Iida, M.; Er, H.; Hisamatsu, N.; Tanase, T. *Chem. Lett.* **2000**, 518. (d) Ikeda, Y.; Imae, T.; Hao, J.-C.; Iida, M.; Kitano, T.; Hisamatsu, N. *Langmuir* **2000**, *16*, 7618.

Table 1. Preparation of P3HT Nanocomposites

P3HT solution (mL)	Ag nanoparticle solution (mL)	weight fraction of Ag in the composite	designation according to Ag nanoparticle (wt %) in the composite
9	1	0.1	Ag10
7.5	2.5	0.25	Ag25
5	5	0.5	Ag50
2.5	7.5	0.75	Ag75
1	9	0.9	Ag90

amine)$_2$]NO_3 complex was extracted into chloroform from the water/chloroform system and recrystallized from ethanol (yield 65%). The composition of the complex was determined by an elemental (CHN) analysis.

(b) Synthesis of Amine-Protected Silver Nanoparticle. The nanoparticle was synthesized by a two-phase redox reaction, which was carried out in the $CHCl_3$/water system using sodium borohydride as a reducing agent. Five milliliters $CHCl_3$ solution of silver amine complex (0.092 mM) and 5 mL of a freshly prepared solution of $NaBH_4$ (0.92 mM) were mixed together and stirred vigorously for 2 h.The excess concentration of $NaBH_4$ converts all the Ag complex into Ag nanoparticle. Subsequently, the mixture was allowed to separate into two distinct transparent phases. A deep-yellow chloroform phase was in equilibrium with a colorless aqueous phase. The chloroform phase was separated and used for the characterization of nanoparticles. The colloidal solution of the nanoparticles was used for making the nanocomposites.

(c) Preparation of the Nanocomposite. Ten milligrams of P3HT (H−T regioregularity 92 mol %, $M_w = 87000$, Aldrich Chem. Co.) was dissolved in 5 mL of $CHCl_3$ and was stirred for 2 h to make the P3HT completely soluble. The P3HT and silver nanoparticle solutions were mixed in different volume ratios given in Table 1 to obtain Ag10, Ag25, Ag50, Ag75, and Ag90 samples where the latter number indicates the weight percentage of Ag in the Ag−P3HT composites. After stirring the mixture for 1 h, we obtained a resultant homogeneous solution and thin films were prepared by spin-casting the P3HT/silver nanoparticle solution onto a glass substrate at a speed of 2000 rpm (Ducom Photoresist Spinner).

(d) Electron Microscopy. The size, shape, and dispersity of the silver nanoparticles in the polymer matrix was studied using transmission electron microscopy (TEM JEOL, 2010EX) operated at an accelerated voltage of 200 kV. A specimen for the transmission electron microscopy (TEM) of the nanoparticle and of the composites were prepared by spreading a small drop of chloroform solution on a carbon-coated copper grid and allowing the drop to dry completely in air. The size distribution of nanoparticles is shown from histograms derived from about 50 particles.

(e) AFM Study. The morphology of dried films of P3HT and the composites were determined using atomic force microscopy (AFM, Model No. Ap0100). AFM instrument was used in the non-contact mode at a resonance frequency of tip end ~300 kHz. The sample was casted on a glass slide from its $CHCl_3$ solution in the AFM. Similar objects formed by a primary surface focusing step were further scanned and the pictures were taken in amplitude mode.

(f) Wide Angle X-ray Scattering (WAXS). The WAXS experiments were carried out on dry powder of the amine capped silver nanoparticles (obtained by the evaporation of solvent from the colloidal solution) using a Seifert X-ray diffractometer (C3000) in reflection mode with a parallel beam optics attachment. The instrument was operated at a 35 kV voltage and a 30 mA current and was calibrated with a standard silicon sample. Nickel filtered copper Kα radiation ($\lambda = 0.154$ nm) was used in the work. The samples were scanned from $2\theta = 30-60°$ in the step scan mode (step size 0.03°, preset time 2 s) and the diffraction pattern was recorded using a scintillation counter detector. An X'Pert PRO (PANalytical) diffractometer, operated at 45 kV voltage and 40 mA current, was used for grazing incidence diffraction. Cu Kα radiation was used in the work.

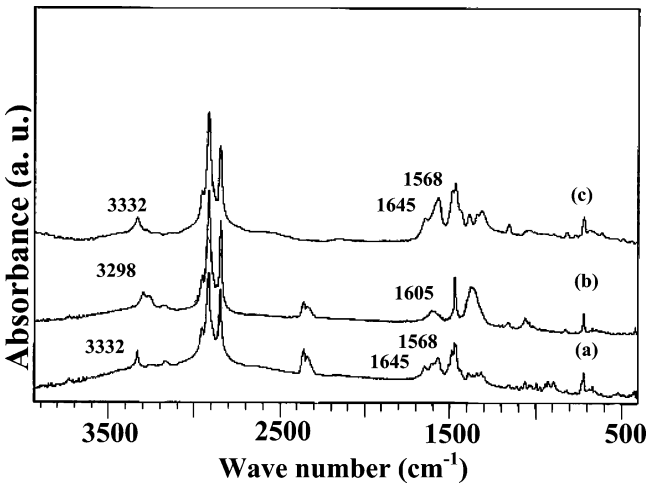

Figure 1. FTIR spectra of (a) hexadecyl amine, (b) silver−amine complex, and (c) silver nanoparticles.

(g) Spectral Characterization. Fourier transform infrared (FT-IR) spectra in the region of 4000−400 cm^{-1} were recorded at room temperature in a Shimadzu FTIR instrument [FTIR-8400S Shimadzu). A specimen for the analysis was prepared as a KBr pellet of dry materials (obtained by the evaporation of solvent from the colloidal solution).

Optical measurements in the solution state were carried out at room temperature on a UV−vis spectrophotometer (Hewlett-Packard, model 8453) from 300 to 1000 nm using a quartz cell (10 mm path length). The spectra were subtracted by the background UV−vis spectra of the same solvent. The UV−vis spectra in the solid state were made from the thin film prepared by spin-casting of the chloroform solution on a glass substrate. The spectra were taken against air at 30 °C in a UV−vis spectrophotometer (Hewlett-Packard, Model 8453) from 300 to 1000 nm.

The photoluminescence experiments of the above spin-cast thin films were performed in a Horiba Jobin Yvon (Fluromax-3) luminescence spectrometer. The photoexcitation was made at an excitation wavelength of 490 nm at a 45° angle of the thin film plane with the excitation beam. The PL spectra of the solutions were performed taking the solution in a quartz cell of path length 1 cm.

(h) Current (*I*)−Voltage (*V*) Measurement. Thin films were cast from the silver nanoparticle solution, P3HT solution, and composite solutions on thoroughly cleaned ITO-coated glass substrate at the speed 2000 rpm. The samples were dried at 60 °C for an additional 3 h in a vacuum oven for complete removal of the solvent. A layer of Al was deposited on the thin film to act as the top electrode. The $I-V$ characteristics of the samples were measured using a dc source electrometer (Keithley model 617) by interfacing with a personal computer.

Results and Discussion

(a) Formation of Metal−Amine Complex and Ag Nanoparticle. Figure 1 shows the FTIR spectra of (i) free amine, (ii) metal−amine complex, and (iii) the composite nanoparticles. The bands at 3332, 3257, and 3170 cm^{-1} are assigned to the NH_2 stretching, NH stretching, and one overtone mode, respectively.[17] The positions of these bands change (3332 → 3298, 3257 → 3266, and 3170 → 3175 cm^{-1}) during complex formation and this shift is due to the

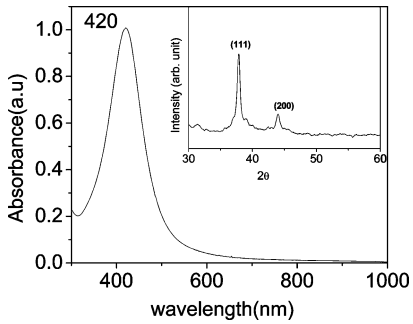

Figure 2. UV−vis spectra of hexadecyl amine capped Ag nanoparticle in $CHCl_3$ solution. [Inset: WAXS pattern of dried hexadecyl amine capped Ag nanoparticle.]

coordination of hexadecyl amine molecule with Ag^+ in the complex. The NH_2 and NH deformation peaks at 1644 and 1568 cm^{-1} also changes similarly to the NH_2 and NH stretching peaks. The interaction of amine group with Ag nanoparticle is negligible, causing almost no change in the stretching frequency of the free amines. The peak positions of CH_3 asymmetric stretching (2957), CH_2 antisymmetric stretching (2919), symmetric stretching (2850), and CH_2 scissoring (1468) vibration modes are invariant both during complex formation and also during nanoparticle formation. Some other bands, e.g., 1568, 1341, 1315, 937, and 901 cm^{-1} peaks, are absent in the spectrum of the complex and it may be due to the preferred arrangement of the amine molecules in the complex. The variation of the infrared absorption band especially for NH and NH_2 bands between the complex and metal nanoparticles suggest the formation of ligand-encapsulated nanoparticle.[17] The structure of the amine group on the metal nanoparticle is like the free amine group and probably the electrostatic interaction of the surface charge of silver nanoparticles and the $-NH_2$ dipoles bind the amine molecules surrounding the nanoparticle surface.

Figure 2 shows the UV−vis absorption spectra of the hexadecylamine protected silver nanoparticle in $CHCl_3$. Here, the surface plasmon absorption band of the nanoparticle is very sharp at 420 nm, indicating a smaller size and narrow size distribution of the Ag nanoparticle.[34] The shape of the plasmon bands are almost symmetrical, suggesting the nanoparticles are well-dispersed and spherical-shaped since the aggregation of the nanoparticle and elongated nanoparticle lead to a broad absorption peak at higher wavelength and the splitting of a plasmon band into two bands, respectively.[35,36]

In the inset of Figure 2, the XRD pattern of the nanoparticle is presented. The two peaks with 2θ values of 38 and 44.5° correspond to two crystal planes, 111 and 200, of metallic crystalline silver, respectively.[37] The broadening in diffraction peaks indicates that the product consisted of small metallic particles.[38]

(b) Characteristics of P3HT−Ag Nanocomposite. (i) UV−Vis Study. The UV−vis spectra of different nanocomposite solutions are shown in Figure 3. The silver nanoparticle solution shows a peak at 420 nm whereas the pure P3HT solution gives a peak at 449 nm due to the $\pi-\pi^*$ transition of conjugated chain. Now the different composite solutions give peaks at 421, 421, 429, 441, and 449 nm for Ag90, Ag75, Ag50, Ag25, and Ag10, respectively. The intensity of the plasmon band of silver nanoparticle decreases with a decrease in silver nanoparticle concentration at different compositions. These results signify that Ag nanoparticle and P3HT mix homogeneously in the solution state, causing fruitful interaction of plasmon band and $\pi-\pi^*$ transition band of P3HT. This interaction of electronic bands produces a single peak in the complex solution spectrum.

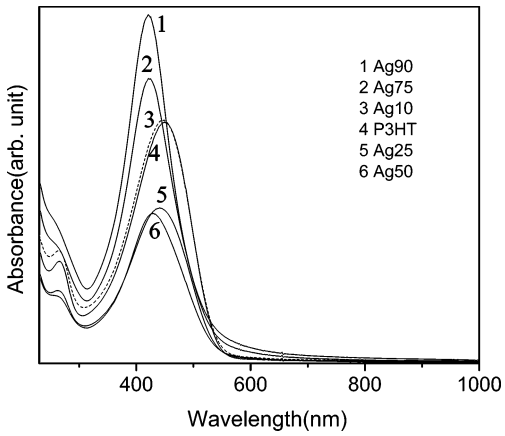

Figure 3. UV−vis spectra of the hexadecyl amine capped Ag nanoparticle−P3HT composites in $CHCl_3$ solution for indicated compositions.

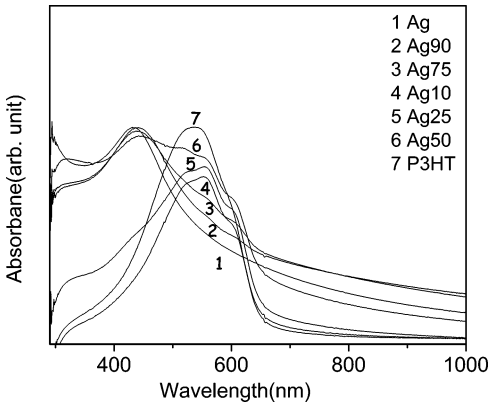

Figure 4. UV−vis spectra of the hexadecyl amine capped Ag nanoparticle composites in thin film for indicated compositions.

On the other hand, thin films of the nanoparticle solution cast on a glass surface give a relatively broad absorption band at 432 nm (Figure 4). The shift to the longer wavelength and broadening of the surface plasmon absorption band of dried thin film compared to that in the solution state may be induced from the agglomeration of silver nanoparticles and/or change of the dielectric properties of the surrounding environment in the thin film state.[34] From the UV−vis spectra of the nanocomposite thin films (Figure 4), it is evident that unlike the spectra at the solution state (Figure 3) the absorption of a plasmon resonance peak of silver nanoparticle (432 nm) and the $\pi-\pi^*$ transition peak of P3HT

(34) Mbhele, Z. H.; Salemane, M. G.; Vansittert, C. G. C. E.; Nedeljkovic, J. M.; Djokovic, V.; Luyt, A. S.; *Chem. Mater.* **2003**, *15*, 5019.
(35) Zheng, J.; Stevenson, M. S.; Hikida, R. S.; Gregory Van Patten, P. *J. Phys. Chem. B* **2002**, *106*, 1252.
(36) Mayer, A. B. R.; Mark, J. E. *Polymer* **2000**, *41*, 1627.
(37) Sun, Y.; Yin, Y.; Mayers, B. T.; Herricks, T.; Xia. Y. *Chem. Mater* **2002**, *14*, 4736.
(38) Yin, Y.; Xu, X.; Xia, C.; Ge, X.; Zhang, Z. *Chem. Commun.* **1998**, 941.

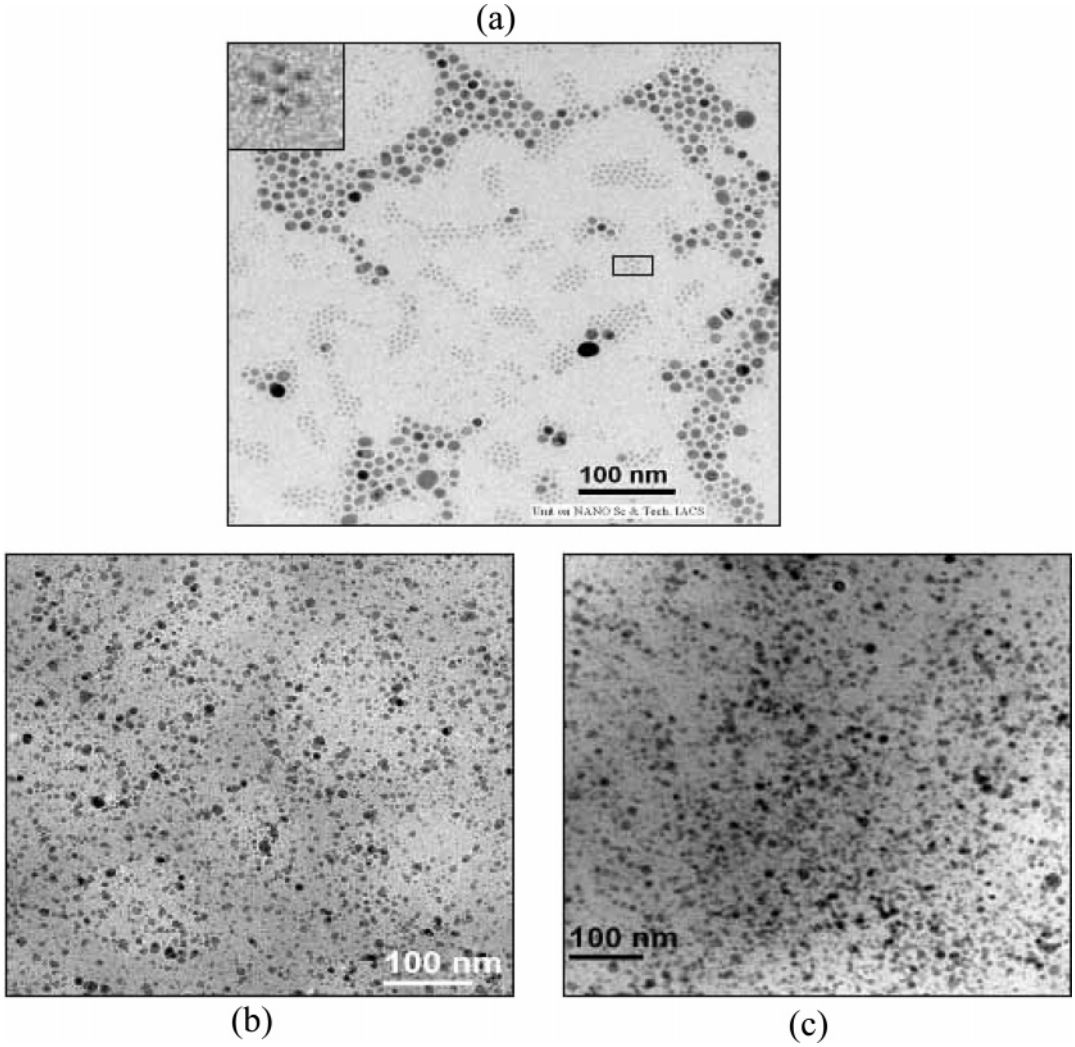

Figure 5. TEM pictures of hexadecyl amine capped silver nanoparticle and composites. (a) Hexadecyl amine capped Ag nanoparticles (inset: enlarged figure shows tha hexagonal close packed arrangement of Ag nanoparticle); (b) Ag25 and (c) Ag50.

(537 nm) coexist in the same spectra. The 600 nm hump of P3HT arising from the vibronic coupling of the $\pi-\pi^*$ transition band[39] remains almost undisturbed in the composites. The intensity of the plasmon band decreases with a decrease in silver concentration in the different nanocomposites and the same is true for the $\pi-\pi^*$ transition peak of P3HT with decreasing P3HT concentration. In the composite film of Ag90 and Ag75 the peak positions of the plasmon band shift to 441 and 439 nm, respectively. This is probably due to the different type of assembly of the silver nanoparticle in the polymer matrix than that in its pure state. At these compositions the $\pi-\pi^*$ transition peak of P3HT shows humps at 556 and 553 nm for Ag90 and Ag75, respectively. In Ag50 the nanoparticle plasmon resonance peak shifts to 441 nm and the $\pi-\pi^*$ transition peak shows doublet humps at 518 and 553 nm. The reason might be due to the effective interaction of the silver nanoparticle with the π electrons in the polymer chain at the 1:1 composition (by weight), causing the plasmon band transition at lower energy. The Ag10 and Ag25 samples show $\pi-\pi^*$ transition peak as a doublet at 553 and 524 nm. The origin of the doublets of the $\pi-\pi^*$ transition peak of P3HT in the P3HT-rich nanocomposites is not known and might be due to the interaction between silver nanoparticle and P3HT, causing easier vibronic coupling.[27] It is to be noted that the $\pi-\pi^*$ transition peak of P3HT at higher P3HT content (Ag75 and Ag90) has red-shifted from 537 to 553 nm. This is probably due to the more ordered structure of P3HT lamella induced by the nanoparticles. The difference of behavior of UV−vis spectra in the solution state and that in the thin film state may be due to the easier movement of the components causing isotropic coupling of plasmon band and $\pi-\pi^*$ transition band in the former state.

(ii) Morphology and Structure. TEM Study. To study the stability of the nanoparticle in the polymer matrix and to analyze the size distribution of the nanoparticle in the pristine form as well as in the composite, we performed a TEM study. Figure 5a shows the TEM image and Figure 6a shows the size distribution of pristine nanoparticles formed from the metal−ligand complex. The particles are spherical and the average size, its standard deviation, and edge−edge separation between particle cores are calculated and its values are respectively 6.9, 2.8, and 2.9 nm, respectively. From the histogram it is evident that the maximum number of particles

(39) Rughoopath, S. D. D. V.; Hotta, S.; Heeger, A. J.; Wudl, F. *J. Polym. Sci., Polym. Phys. Ed.* **1987**, *25*, 1071.

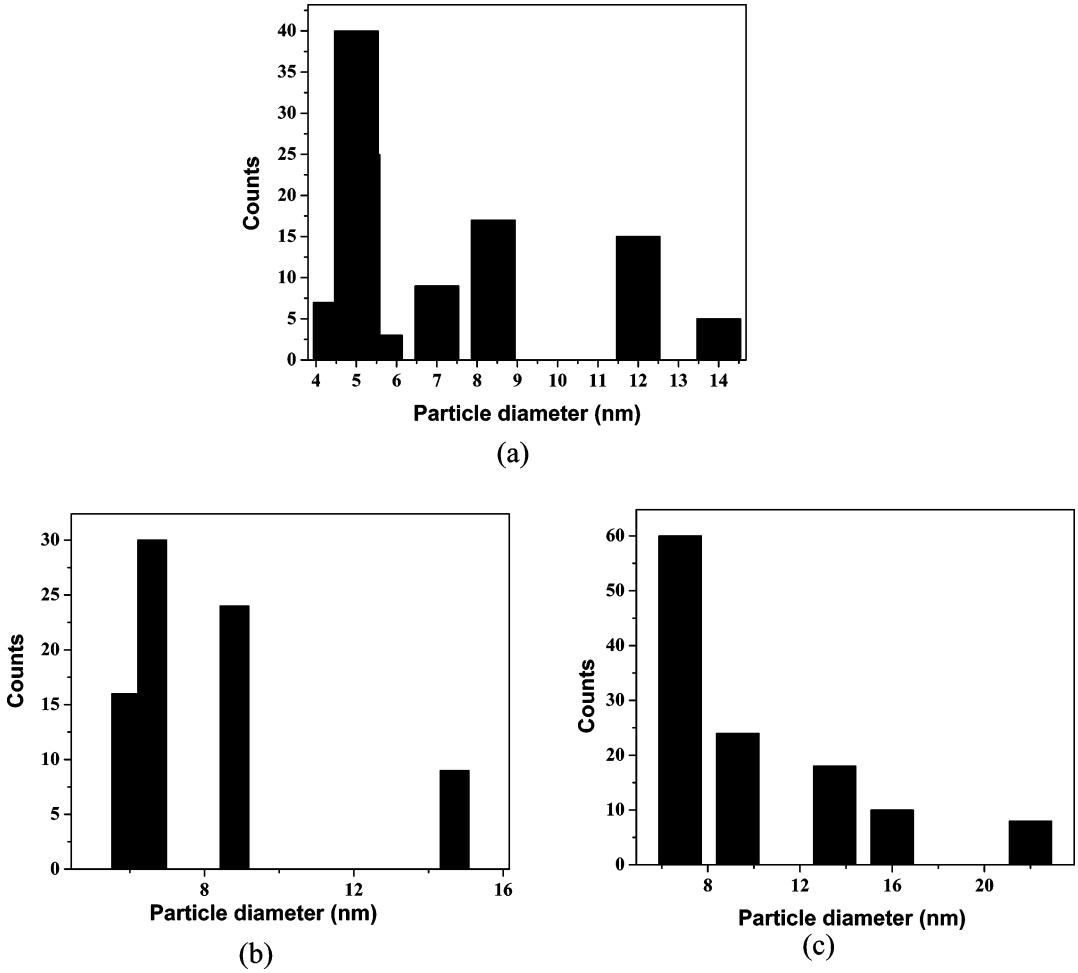

Figure 6. Histogram of (a) hexadecyl amine capped Ag nanoparticle, (b) Ag25, and (c) Ag 50.

have the average size around 5 nm. These amine-coated particles have a very well defined nanoassembly instead of aggregation of the metal cores into larger particles or flocs. The nanoscale structure formed by these small particles follows a two-dimensional hexagonal array (inset of Figure 5a) with a constant edge−edge separation between silver cores. From the histogram it is also seen that there are some particles having the diameter 7, 8.5, 12, and 14 nm. These particles do not strictly follow the hexagonal two-dimensional arrangement as observed in case of particles of 5 nm diameter.

Figure 5b and 5c shows the TEM images of Ag25 and Ag50 composite materials, respectively. It is clear from the TEM images that the nanoparticles are well-dispersed and stable in the polymer matrix. The histograms of the two composites Ag25 and Ag50 are shown in Figure 6b and 6c. From the histograms it is evident that as the percentage of nanoparticle in the composite increases, the average diameter of the particles increases. The average sizes of silver nanoparticles are 6.9 ± 2.8, 8.0 ± 2.7, and 9.0 ± 4.4 nm for pure Ag, Ag25, and Ag50, respectively. This increase is due to the aggregation of the individual smaller nanoparticles into a bigger dimension as the concentration of the colloidal silver increases in the composites. For lower Ag nanoparticle concentration the nanoparticles are more homogeneously dispersed in the composite film, but at higher Ag nanoparticle concentration some nanoparticles aggregate to produce bigger size particles. It is to be noted from Figure 6 that size distributions of nanoparticles are discrete in nature and might arise from the agglomeration of two or more nanoparticles, leaving the intermediate diameter vacant. Although the Ag nanoparticles are well-stabilized by the amine molecule, the hexyl side chains of P3HT may interact with the hydrophobic part of the Ag nanoparticle (amine molecule), creating a different nature of the assembly. Increasing Ag−nanoparticle concentration may cause aggregation of such nanoparticle assembly in the polymer matrix, resulting in an increase of the average nanoparticle size.

AFM Study. AFM study of the pristine film of P3HT and the nanocomposites (Figure 7) are carried out to investigate any morphology change that occurs from P3HT to the composite film. The pristine film of P3HT is uniform and flat, containing some fibril-like morphology on the surface (fibrillar diameter $\sim$ 20 nm). The different composite films show uniform morphology containing clumps of bigger dimensions. The clumps are produced by the aggregation of P3HT lamella surrounding the nanoparticle surface. The average dimension of the domain that was formed by the nanoparticle and the P3HT lamella aggregation increases with increase in nanoparticle concentration. This is probably due to the multilayer aggregation of the lumps of Ag nanoparticles and P3HT.

Thickness Measurement. The thicknesses of the thin films of the nanocomposites measured from a Veeco Dektak

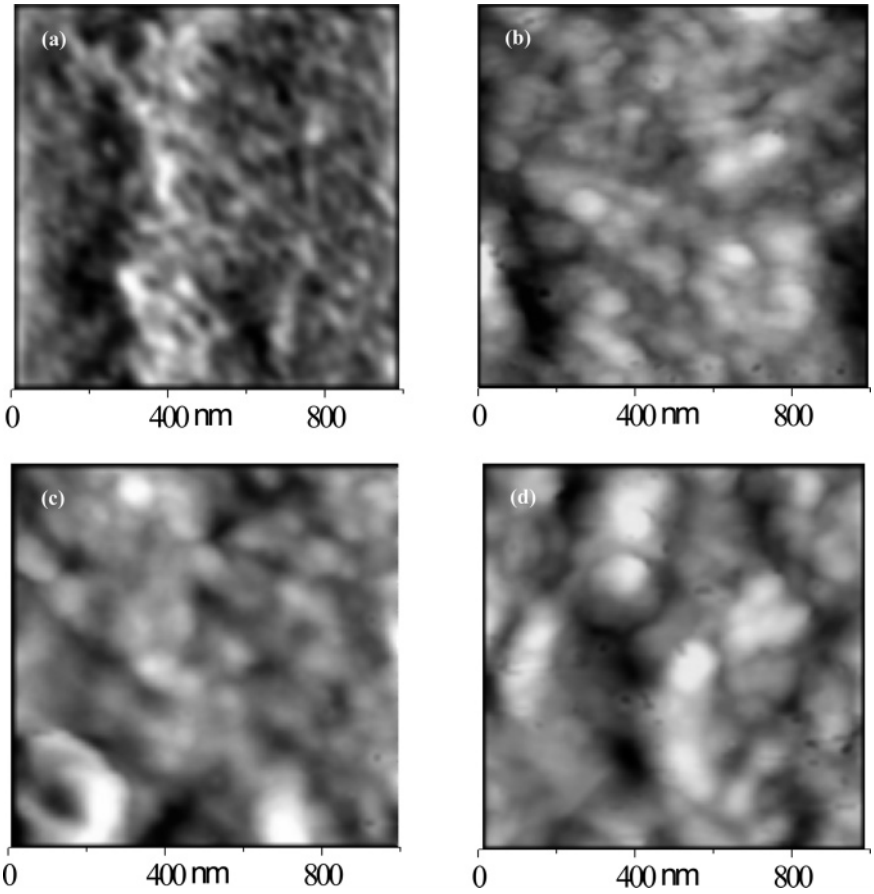

Figure 7. AFM pictures (height image) of (a) P3HT, (b) Ag25, (c) Ag50, and (d) Ag75.

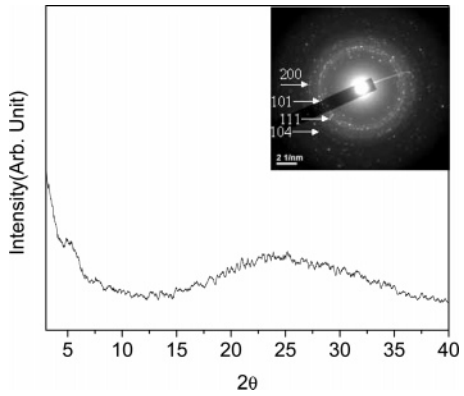

Figure 8. Grazing incidence X-ray diffractogram Ag50 thin film (inset: electron diffraction of the same sample).

profilemeter are 39, 40, 42, 51, 62, and 64 nm for P3HT, Ag10, Ag25, Ag50, Ag75, and Ag90, respectively. It is evident from the data that as the Ag nanoparticle concentration increases, the thicknesses of the thin films cast under similar conditions increase. Probably the insertion of more layers of silver nanoparticle into the P3HT matrix with increasing nanoparticle concentration causes such an increase in the thickness of the thin films. Also the increase of average nanoparticle size with increase in Ag concentration might be another reason for the increasing thickness of the thin films.

Grazing Incidence X-ray and Electron Diffraction. Figure 8 shows a characteristic grazing incidence X-ray diffractogram and electron diffractogram of a Ag50 composite sample. The X-ray diffractogram clearly indicates lamellar structure of P3HT. However, no peak characterizing type-1or type-2 polymorph[40] of P3HT crystal is observed. In the electron diffractogram of Ag50 there are spots producing concentric rings, indicating a polycrystalline nature of Ag in the composite. Analysis of the data indicates the presence of d_{hkl} values, 2.46, 2.31, 2.02, and 1.74 Å for 101, 111, 200, and 104 Miller planes of metallic Ag (JCPDS International Center for Diffraction Data). It is evident from Figure 8 that the diffraction peaks of Ag are absent in the X-ray data of the thin film. So from these results it may be concluded that P3HT is present as lamella but the crystalline nature is not known. It might be mesomorphic in nature,[23] as in the electron diffraction pattern no diffraction pattern of P3HT (d = 3.8 and 4.3 Å)[40] crystal is present. In Figure 9 a schematic model of hexadecyl amine capped Ag nanoparticle encapsulated by P3HT lamella is presented. Some interaction of dispersion type between the interdigitated cetyl chains of Ag nanoparticle with hexyl side chains of P3HT is possible. The model of the unit repeats to produce P3HT lamella surrounding the nanoparticle and its layer-by-layer deposition causes clump formation of the composite.

(iii) Photoluminescence (PL) Spectra. Steady-state PL was recorded after exciting the composite solutions and the pristine P3HT solution with a 500 nm laser. Figure 10 shows the solution-state PL spectra of the P3HT and the composite solution in $CHCl_3$. From the PL spectra it is clear that the photoluminescence intensity of the composite solution

(40) Prosa, T. J.; Winokur, M. J.; McCullough, R. D. *Macromolecules* **1996**, *29,* 3654.

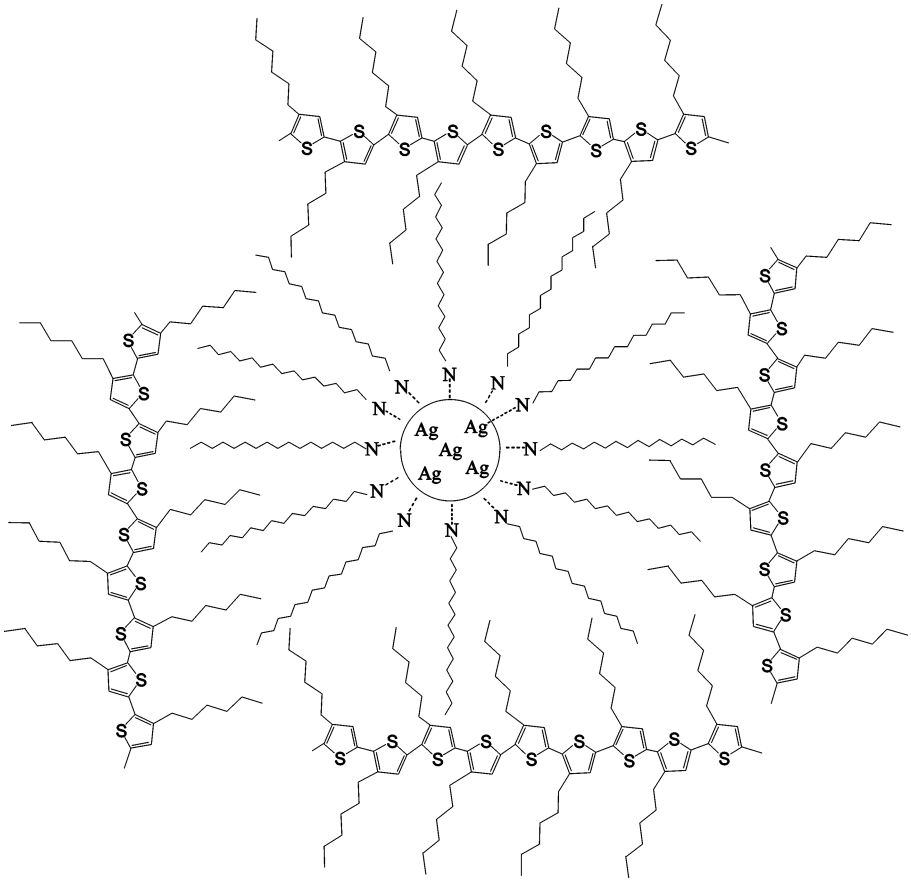

Figure 9. Schematic model of the hexadecyl amine capped Ag−P3HT nanocomposite. (Dotted lines indicate physical bonding between Ag nanoparticle and nitrogen atom of amine group. Repetitions of the unit produce P3HT lamella and multilayered Ag−P3HT nanocomposite.)

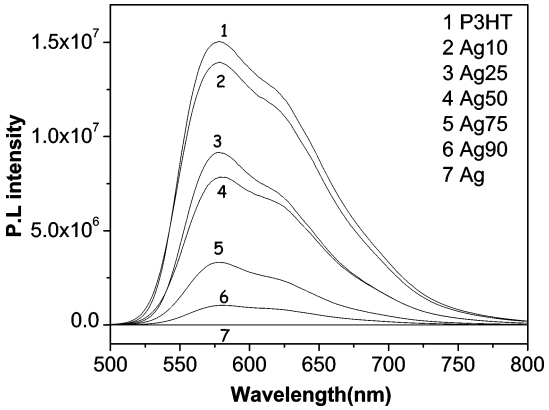

Figure 10. Photoluminescence spectra of the nanocomposites in $CHCl_3$ solution for indicated compositions.

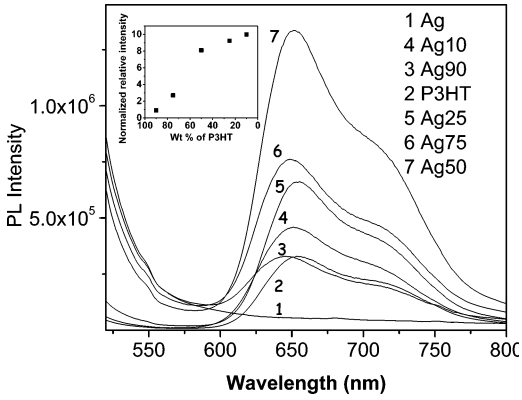

Figure 11. Photoluminescence spectra of the hexadecyl amine capped Ag nanoparticle composites in thin film for indicated compositions. [Inset: Relative increase of PL intensity normalized with the amount of P3HT content in different composite thin films.]

decreases with increase in silver nanoparticle concentration, as the latter shows no photoluminescence in chloroform. It may be noted that the composite solutions do not show any substantial peak shift, indicating that the nanoparticles have no effect on the excited state of the P3HT molecule. Figure 11 shows the PL spectra of the thin films of the P3HT and the composites of different compositions. It is evident from the figure that the P3HT luminescence is greatly enhanced by the addition of nanoparticle and the composite film Ag50 shows the highest PL intensity, i.e., about a 4 times increase in the PL intensity (8 times increase in the PL intensity when normalized with weight of P3HT) compared to that of P3HT. The Ag75 composite also shows higher PL intensity than that of P3HT film. The Ag90 composite shows almost equal PL intensity with P3HT though it contains only 10% of P3HT by weight. The inset of Figure 11 shows the plot of a relative increase in the PL intensity normalized with the amount of P3HT content in different composite thin films. A sharp increase of PL intensity indicates that Ag nanoparticles has strong interaction with the excited state of P3HT in the solid state.

For the excitation wavelength at 500 nm the thin films show an emission at 654, 652, 653, 652, 649, and 646 nm for P3HT, Ag10, Ag25, Ag50, Ag75, and Ag90, respectively. So in the nanocomposites PL band exhibits a blue shift and the effect is more pronounced for Ag75 and Ag90. The blue shift of the emitted band may be attributed to the coupling

of the plasmon band of the low-dimensional silver nanoparticles with π-electrons of P3HT.[41] In the case of Ag75 and Ag90 the concentration of silver nanoparticle is very high, so the coupling effect of the lower dimension nanoparticles causing the blue shift of the photoluminescence band is more pronounced.

The Ag nanoparticle thin film does not show luminescence; therefore, the enhancement of photoluminescence intensity in the film is clearly linked with the inclusion of silver nanoparticle into the P3HT matrix. The enhancement may be attributed to two reasons: (i) the addition of silver nanoparticle effectively increases the amount of incident light by reflection from each nanoparticle, thereby increasing the path length; consequently, the population of excitons in P3HT increases, resulting in enhancement of PL intensity. The structural features of nanoparticles could play a critical role, as size, shape, and concentration of the metallic nanoparticles may have a direct influence on the reflection of incident light. (ii) Another reason for photoluminescence enhancement is the effect of silver nanoparticle as a spacer between P3HT chains. An increase in chain separation would result in enhanced intrachain character of the photogenerated excitons, and consequently an increase in the photoluminescence intensity occurs due to decrease of decaying path.[42] The photoluminescence quenching in the nanocomposite solutions is due to the increased decaying path for increased nonradiative decay from the solvent molecules. Also, increased intermolecular collision of the components from easier thermal motion in the solution than that in the thin film may be another cause.

Currrent−Voltage ($I-V$) Behavior. The $I-V$ characteristics of the thin film device formed from P3HT, silver nanoparticle, and different nanocomposites are presented in Figure 12a and 12b). In Figure 12a the $I-V$ characteristics recorded by scanning from (i) 0 to +3 V and then (ii) +3 to −3 V followed by a reverse scan (iii) from −3 to +3 V are presented. The figure represents nonlinear characteristics and the curves indicate an electrical bistability. The current is about 25 times higher during the sweep from +3 to −3 V and represents a switching behavior.[43] Here, the memory phenomenon as well as the reproducibility of the device by running three consecutive loops from +3 to −3 V is clearly observed. The $I-V$ characteristic curve traces almost the same path of its predecessors. In the negative bias direction it is observed that at a particular voltage there exist two different conducting states (bistability). With scanning from the positive to negative bias direction, the current is as low as 10^{-4} μA (off state), but when −3 V is reached, the current jumps to a very high value, 25 μA (on state). With scanning back from −3 V toward +3 V, the system comes down to the off state at a suitable forward bias. This procedure when continued further follows the same nature and thus the reproducibility is evident. The mechanism for the bistability behavior may be due to the charge confinement by the

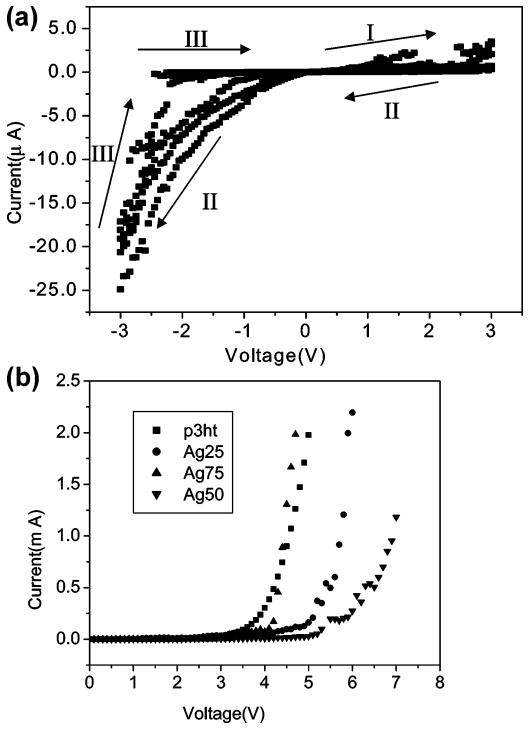

Figure 12. (a) $I-V$ characteristic curves of the hexadecyl amine capped Ag nanoparticle thin film for three consecutive cycles. (b) $I-V$ characteristic curves of different composite thin films at indicated compositions.

nanoparticle in the amine capped silver nanoparticle assembled thin film.[43,44] These nanoparticles start to be charged at a suitable negative bias by obtaining the electrons from the Al electrode and this charge gets a percolating path through the channels of nanoparticles and gives a very high current in the device. This continues until all the nanoparticles become charged. Once all the particles become charged, the device reaches the low conducting off state as the cause of charge flow becomes negligible. In this way charging and discharging continues showing switching behavior.

Figure 12b shows the $I-V$ characteristics of P3HT and its composites. The inflection voltage of conduction increases with increase in silver nanoparticle concentration up to Ag50 and then it decreases for Ag75. It means that at lower nanoparticle concentration the nanoparticle hinders the flow of electron and hole. Because the nanoparticle domain isolates the polymer chains, it can be qualitatively argued that electrons and hole could be effectively confined within the domains of polymer chain separated by nanoparticles. The probability of exciton formation by bipolar recombination would therefore increase in all the devices, promoting their behavior as efficient LEDs.[45] These excitons confined in the nanodomain (quantum well) produced by the assembly of the nanoparticle in the polymer matrix perform singlet decay before losing their energy via a nonradiative decay. So we can expect that the electroluminescence intensity will abruptly increase with increase in silver concentration similar to the PL (Figure 10). From these $I-V$ characteristics it can

(41) Selvan, S. T.; Hayakawa, T.; Nogami, M. *J. Phys. Chem. B* **1999**, *103*, 7064.
(42) Lee, T.-W.; Park, O. O.; Kim, J.-J.; Hong, J.-M.; Kim, Y. C. *Chem. Mater.* **2001**, *13*, 2217.
(43) Tseng, R. J.; Huang, J.; Ouyang, J.; Kaner, R. B.; Yang, Y. *Nano Lett.* **2005**, *5*, 1077.
(44) Wang, H. P.; Pigeon, S.; Izquierdo, R.; Martel, R. *Appl. Phys. Lett.* **2006**, *89*, 183502.
(45) Ohmori, Y.; Uchida, M.; Muro, K.; Yoshino, K. *Solid State Commun.* **1991**, *80*, 605.

be inferred that all the devices would behave as efficient light-emitting diodes.[45,46] In the case of Ag75 composite the current increases after 4.4 V (near the pure P3HT) and after this voltage it gives more current than that of pure polymer. It may be due to the hopping of electrons through the denser metallic islands in this composite.

Conclusion

Five Ag−P3HT nanocomposites of different Ag−nanoparticle concentrations, e.g., Ag10, Ag25, Ag50, Ag75, and Ag90, are prepared by mixing a solution of P3HT and hexyl amine capped silver nanoparticles in $CHCl_3$ medium. The UV−vis spectral data indicate homogeneous mixing of the components in the solution state because the plasmon band and $\pi-\pi^*$ transition band yield an intermediate peak in each case. But in the solid state the plasmon band of silver and $\pi-\pi^*$ transition band of P3HT are observed separately, though a small red shift of plasmon band and $\pi-\pi^*$ trasition band are observed at certain compositions. TEM study indicates homogeneous distribution of Ag nanoparticles in the composite and the histogram indicates increase of average diameter of Ag nanoparticle with increase in Ag nanoparticle concentration. The distribution of nanoparticle in P3HT film is discrete in nature, indicating the differently sized nanoparticles are produced from the aggregation of a different number of nanoparticles. AFM study indicates that in the composite clumps are produced by the aggregation of P3HT lamella surrounding the silver nanoparticles. In the solution state the photoluminescence spectra show a decrease in photoluminescence intensity with increase in silver nanoparticle concentration but in the thin films the photoluminescence intensity increases dramatically with increase in silver nanoparticle concentration. The emission peaks in the thin films also show a small blue shift with increase in silver nanoparticle concentration. The thin films of pure hexadecyl amine capped silver nanoparticles have two different conductivity states (bistability), exhibiting switching behavior. On the other hand, the $I-V$ characteristic curves of nanocomposite thin films exhibit a characteristic of light-emitting diodes. The threshold voltage for the inflection of current increases with increase in nanoparticle concentration up to Ag50, and for Ag75 the threshold voltage is almost equal to that of pure P3HT. Thus, the thin films of Ag−P3HT nanocomposites are promising materials for fabrication of novel optical and more efficient light-emitting diodes than that of pure P3HT.

Acknowledgment. We gratefully acknowledge the Council of Scientific and Industrial Research for granting a fellowship. The CSIR Grant No. 01-(1919)/04 EMR-II and 01-(1919)/04/EMR-II are gratefully acknowledged for financial support. Financial support from the Department of Science and Technology under the Nanoscience and Nanotechnology Programme is also gratefully acknowledged.

CM7020214

(46) Burroughes, J. H.; Bradley, D. D. C.; Brown, A. R.; Marks, R. N.; Mackay, K.; Friend, R. H.; Burns, P. L.; Holmes, A. B. *Nature* **1990**, *347*, 539.